ADVANCED ENERGY MATERIALS
www.advenergymat.de

Highly Efficient Polymer Tandem Cells and Semitransparent Cells for Solar Energy

Chih-Yu Chang, Lijian Zuo, Hin-Lap Yip, Chang-Zhi Li, Yongxi Li, Chain-Shu Hsu, Yen-Ju Cheng, Hongzheng Chen,* and Alex K-Y. Jen**

Highly efficient tandem and semitransparent (ST) polymer solar cells utilizing the same donor polymer blended with [6,6]-phenyl-C_{61}-butyric acid methyl ester ($PC_{61}BM$) and [6,6]-phenyl-C_{71}-butyric acid methyl ester ($PC_{71}BM$) as active layers are demonstrated. A high power conversion efficiency (PCE) of 8.5% and a record high open-circuit voltage of 1.71 V are achieved for a tandem cell based on a medium bandgap polymer poly(indacenodithiophene-co-phananthrene-quinoxaline) (PIDT-phanQ). In addition, this approach can also be applied to a low bandgap polymer poly[2,6-(4,4-bis(2-ethylhexyl)-4H-cyclopenta[2,1-b;3,4-b′]dithiophene)-alt-4,7-(5-fluoro-2,1,3-benzothia-diazole)] (PCPDTFBT), and PCEs up to 7.9% are achieved. Due to the very thin total active layer thickness, a highly efficient ST tandem cell based on PIDT-phanQ exhibits a high PCE of 7.4%, which is the highest value reported to date for a ST solar cell. The ST device also possesses a desirable average visible transmittance (≈40%) and an excellent color rendering index (≈100), permitting its use in power-generating window applications.

1. Introduction

Organic photovoltaics (OPVs) are of great interest as an alternative renewable energy source to typical silicon-based photovoltaic cells due to their potential for cost-effective large-area manufacturing, light-weight, mechanical flexibility, and semitransparent (ST) characteristics.[1–6] An emerging market segment for OPVs is ST solar cells that can be used for window integration, which permits daylight to pass through while generating electricity.[3–6] Currently, the most efficient OPVs are based on the bulk-heterojunction (BHJ) architecture, in which an electron-donor (e.g., a conjugated polymer) is blended with an electron-acceptor (e.g., [6,6]-phenyl-C_{61}-butyric acid methyl ester ($PC_{61}BM$) or [6,6]-phenyl-C_{71}-butyric acid methyl ester ($PC_{71}BM$)) to form the active layer.[1,2] One of the factors limiting the power conversion efficiency (PCE) of BHJ OPVs is insufficient absorption of solar radiation due to the active layer usually suffers from: 1) narrow absorption bandwidth[1,2] and 2) limited thickness because the low charge carrier mobility of organic semiconductors.[1,2,7] In addition, the thermalization losses of hot charge carriers generated by high energy photons reduce the maximum achievable cell voltage.[8–10] A possible approach to address these issues is to stack individual cells with complementary absorption characteristics into a tandem cell structure.[7–10] This configuration usually consists of a front cell with a large bandgap (E_g) polymer ($E_g > 1.7$ eV), an interconnection layer (ICL), and a rear cell with a low bandgap (LBG) polymer ($E_g < 1.5$ eV).[10] However, the progress in polymer tandem cells is still limited due to lacking of high-performance LBG polymers.[8,9] Additionally, although most of the high-performance single-junction devices reported to date are based on medium bandgap polymers ($E_g \approx 1.6$ eV),[10] their utilization in tandem cells remains quite challenging because their absorption have significant overlap with other commonly used polymers.[10] Considering that $PC_{61}BM$ and $PC_{71}BM$ possess different absorption characteristics in the visible region,[11] the combination of a medium bandgap polymer with $PC_{61}BM$ and $PC_{71}BM$ as the active layer would be an promising approach to realize the complementary absorption characteristics.

In this work, we demonstrate highly efficient tandem polymer solar cells and ST solar cells utilizing the same donor polymer blended with $PC_{61}BM$ or $PC_{71}BM$ as active layers in two sub-cells. The tandem device structure consists of two sub-cells that are electrically connected in series via an ICL of modified poly(3,4-ethylene-dioxythiophene):poly(styrenesulfonate) (hereafter referred to as m-PEDOT:PSS)/high conductivity PEDOT:PSS (hereafter referred to as PH1000)/ZnO films, as illustrated in **Figure 1**a. Two polymers are used in this study:

Dr. C.-Y. Chang, L. Zuo, Dr. H.-L. Yip, Dr. C.-Z. Li, Y. X. Li, Prof. A. K.-Y. Jen
Department of Materials Science and Engineering
University of Washington
Seattle, WA, 98195, USA
E-mail: ajen@u.washington.edu
Dr. C.-Y. Chang, Prof. C.-S. Hsu, Prof. Y.-J. Cheng
Department of Applied Chemistry
National Chiao Tung University
1001 Ta Hseuh Road, Hsin-Chu, 30010, Taiwan
E-mail: cshsu@mail.nctu.edu.tw
L. Zuo, Prof. H. Z. Chen
State Key Laboratory of Silicon Materials
MOE Key Laboratory of Macromolecule Synthesis and Functionalization
Zhejiang-California International Nanosystems Institute
Zhejiang University
Hangzhou, 310027, P. R. China
E-mail: hzchen@zju.edu.cn

DOI: 10.1002/aenm.201301645

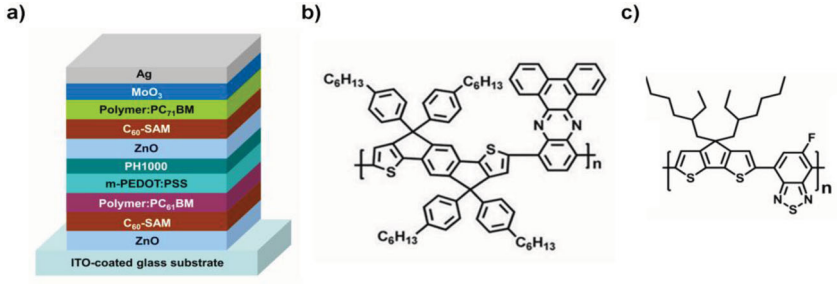

Figure 1. a) Schematic representation of the tandem device architecture used in this study. Chemical structures of: b) PIDT-phanQ and c) PCPDTFBT.

a medium bandgap polymer poly(indacenodithiophene-*co*-phananthrene-quinoxaline) (PIDT-phanQ; chemical structure shown in Figure 1b) and a LBG polymer poly[2,6-(4,4-bis(2-ethylhexyl)-4H-cyclopenta[2,1-b;3,4-b′]dithiophene)-alt-4,7-(5-fluoro-2,1,3-benzothia-diazole)] (PCPDTFBT; chemical structure shown in Figure 1c). The tandem cell based on PIDT-phanQ exhibits a very high PCE up to 8.5%, which is the first demonstration of a tandem cell based on a medium bandgap polymer with such a high PCE. This approach can also be applied to a LBG polymer PCPDTFBT-based tandem cell to achieve a high PCE up to 7.9%. More importantly, the thin active layers used in these tandem cells make them ideal for ST solar cells. A record high PCE of 7.4% with an average visible transmittance (AVT) of ≈40% and a general color rendering index (CRI) of ≈100 could be achieved for PIDT-phanQ-based ST cells.

2. Results and Discussion

2.1. Single-Junction Solar Cells

To achieve highly-efficient tandem solar cells, the optimization of active layer thickness of the sub-cells is critical for balanced light absorption and matched photocurrent.[7–10] Therefore, single-junction devices based on PIDT-phanQ blended with $PC_{61}BM$ or $PC_{71}BM$ (device structure: indium tin oxide (ITO)-coated glass/ZnO/fullerene self-assembled monolayer (C_{60}-SAM)/PIDT-phanQ:$PC_{61}BM$ or $PC_{71}BM$/m-PEDOT:PSS/Ag) were preliminarily studied. A C_{60}-SAM layer was used to passivate ZnO surface traps and enhance electronic coupling between ZnO and the active layer.[12,13] The current–voltage (*J*–*V*) characteristics of the devices were measured under AM1.5 illumination (Supporting Information Figure S1), and the corresponding device parameters were summarized in Supporting Information Table S1. It is clearly shown that PCE decreased when the thickness of the active layer increased (Table S1 and Figure S1) independent from the type of fullerene derivatives used. This is consistent with previous observations that thicker active layer tends to increase bimolecular charge recombination and cause a space charge effect.[2,14,15]

Based on the optimal active layer thickness, Device A with $PC_{61}BM$ acceptor exhibited a short-circuit current density (J_{sc}) of 8.56 mA cm^{-2}, an open-circuit voltage (V_{oc}) of 0.85 V, a fill factor (FF) of 68.56%, and a PCE of 5.0%, which was inferior to that of Device B with $PC_{71}BM$ acceptor (PCE = 6.5%, with a J_{sc} of 11.45 mA cm^{-2}, an V_{oc} of 0.87 V, and a FF of 65.04%), as shown in **Table 1** and **Figure 2**. The good agreement between the measured J_{sc} and that extrapolated from the external quantum efficiency (EQE) spectra confirms the accuracy of the reported PCE values (Table 1). The difference in PCE between Device A and Device B was mainly due to different J_{sc} values (Table 1 and Figure 2), which can be rationalized by comparing the spectral response in the EQE spectra (**Figure 3**a). Device A revealed two dominant peaks at 435 nm and 645 nm (with the maximum EQE of ≈55% at 435 nm), while Device B revealed a broad spectral response in the range between 350 and 700 nm (with the maximum EQE of ≈65% at 540 nm). This distinction was also manifested in the absorption spectra of the blend films (Figure 3b), which can be ascribed to the fact that $PC_{71}BM$ possesses better light absorption in the visible region compared to that of $PC_{61}BM$.[11]

It is worthy noting that both Device A and Device B possessed high FF values (>65%), as shown in Table 1. The reason

Table 1. Summary of the photovoltaic properties of solar cells.

Device	Condition[a)]	V_{oc} [V]	J_{sc} [mA cm^{-2}]	FF [%]	PCE [%]
A	PIDT-phanQ, front cell	0.85	8.56 (8.45)[d)]	68.56	5.0
B	PIDT-phanQ, rear cell	0.87	11.45 (11.24)[d)]	65.04	6.5
C	PIDT-phanQ, tandem cell	1.71	6.91	65.70	7.8
D	PCPDTFBT, front cell	0.75	10.61	62.09	4.9
E	PCPDTFBT, rear cell	0.76	13.90	58.08	6.1
F	PCPDTFBT, tandem cell	1.51	8.39	57.04	7.2
G	PIDT-phanQ, tandem cell[b)]	1.68	5.93	68.58	8.5
H	PCPDTFBT, tandem cell[c)]	1.47	5.75	58.64	7.9
I	PIDT-phanQ, ST cell	1.70	5.81	67.40	6.7
J	PIDT-phanQ, ST cell[b)]	1.63	5.23	68.94	7.4

[a)]Polymer and device architecture; [b)]Light intensity = 80 mw cm^{-2}; [c)]Light intensity = 63 mW cm^{-2}; [d)]Calculated from the EQE spectra shown in Figure 3a.

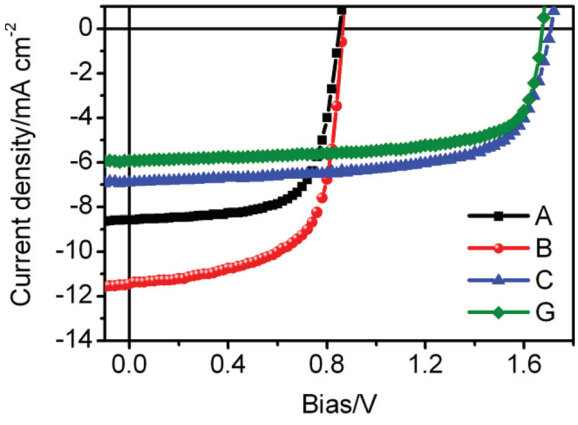

Figure 2. *J*–*V* characteristics of solar cells based on PIDT-phanQ (see Table 1 for descriptions of the device types).

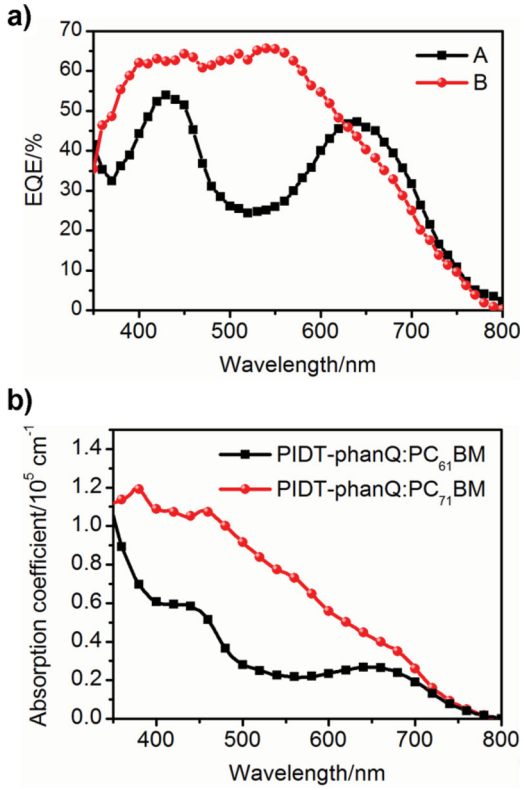

Figure 3. a) EQE spectra of the as-fabricated devices (see Table 1 for descriptions of the device types) and b) absorption spectra of PIDT-phanQ:$PC_{61}BM$ and PIDT-phanQ:$PC_{71}BM$ films.

for the high FF is most probably the thin active layer thickness (≈80 nm), which can decrease the charge carrier recombination losses within the active layer.[1,2] To gain further insight into the effectiveness of the overall photoconversion process within the devices, the internal quantum efficiencies (IQEs) of the devices were evaluated by measuring their total absorption spectra (based on the reflection geometry) and EQE spectra.[6] As shown in **Figure 4**, the IQEs of both devices were remarkably high, with the maximum values approaching 100%, confirming the efficient exciton dissociation, charge transport, and charge collection within the devices.

2.2. Tandem Soar Cells

The device characteristics of a double-junction tandem solar cell comprising a front cell of PIDT-phanQ:$PC_{61}BM$ (70 nm) and a rear cell of PIDT-phanQ:$PC_{71}BM$ (85 nm) was then studied. An ICL consisting of m-PEDOT:PSS/PH1000/ZnO is used to connect the sub-cells effectively because it possesses desired high optical transparency (≈85% in 700–900 nm), reasonable conductivity (≈15 S cm^{-1}), smooth surface (root-mean-square roughness = 0.88 nm), and excellent robustness against solvent erosion.[16] Under the AM1.5G illumination (with an intensity of 100 mW cm^{-2}), Device C showed a high PCE of 7.8%, with a J_{sc} of 6.91 mA cm^{-2}, a FF of 65.70%, and an exceptional V_{oc} of 1.71 V (Table 1 and Figure 2). This represents the highest V_{oc} value reported to date for a double-junction organic tandem cell. This high V_{oc} value is also close to the sum of the V_{oc} of two sub-cells (Table 1 and Figure 2), confirming that they are electronically coupled in series through the ICL. It is worth noting that the measured J_{sc} of the tandem cell (6.91 mA cm^{-2}; Device C in Table 1) agrees well with the predicted value from optical simulation (6.97 mA cm^{-2}), indicating there is no significant electrical loss in the tandem cell.

We have also examined if similar strategy can be used for LBG polymer-based tandem cells. PCPDTFBT was previously proven to be an efficient polymer for OPV, possessing good solubility in common organic solvents, broad absorption band that extends into near IR with an onset of ≈920 nm (E_g = 1.35 eV), high charge carrier mobility (≈10^{-2} cm^2 V^{-1} S^{-1}), and good air stability.[16,17] The optimal PCE for PCPDTFBT:$PC_{61}BM$ (Device D) and PCPDTFBT:$PC_{71}BM$ (Device E) single-junction cells was 4.9% and 6.1%, respectively (Table 1 and **Figure 5**). A double-junction tandem solar cell consisting of a PCPDTFBT:$PC_{61}BM$ (80 nm) front cell and a PCPDTFBT:$PC_{71}BM$ (85 nm) rear cell was fabricated (Device F). Under the AM1.5G illumination (100 mW cm^{-2}), Device F exhibited a high PCE of 7.2%

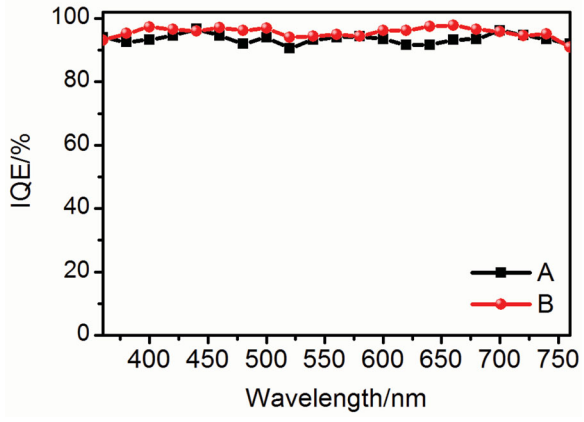

Figure 4. IQE spectra of the as-fabricated devices (see Table 1 for descriptions of the device types).

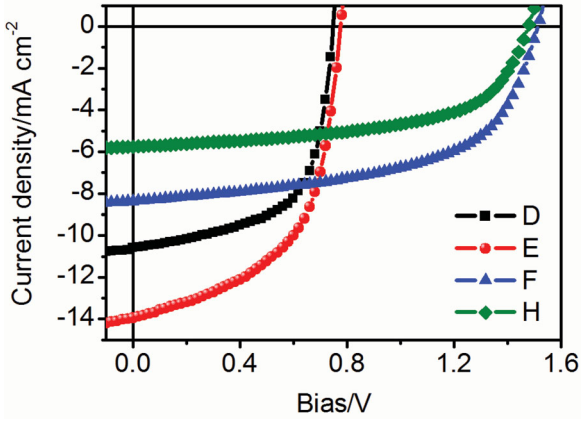

Figure 5. *J–V* characteristics of the solar cells based on PCPDTFBT (see Table 1 for descriptions of the device types).

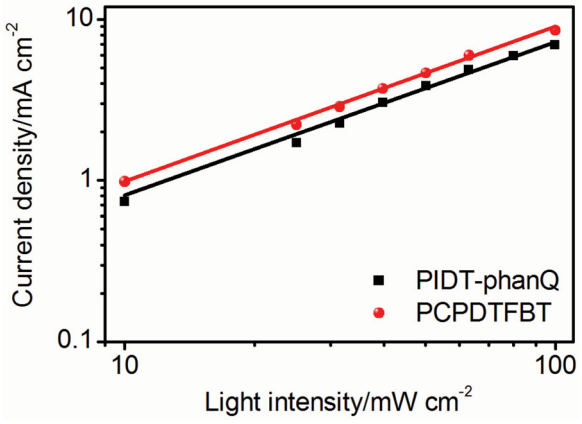

Figure 6. Short-circuit current density plotted against incident light intensity for PIDT-phanQ- and PCPDTFBT-based tandem cells.

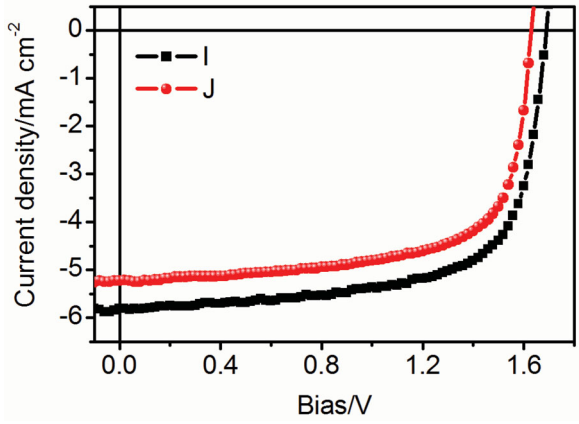

Figure 7. *J–V* characteristics of ST solar cells based on PIDT-phanQ (see Table 1 for descriptions of the device types).

with a J_{sc} of 8.39 mA cm^{-2}, a FF of 57.04%, and an V_{oc} of 1.51 V (Table 1 and Figure 5). These results show the feasibility of using the same donor polymer to blend with $PC_{61}BM$ and $PC_{71}BM$ to serve as active layer in two sub-cells for constructing highly efficient tandem cells.

We also studied the light-intensity dependence of the photocurrent, which can provide the information about which type of recombination (e.g. monomolecular or bimolecular) is dominant and whether space charge effects play a role.[18,19] The short-circuit current densities of PIDT-phanQ- and PCPDTFBT-based tandem cells as function of light intensity are shown in **Figure 6**. For both devices, we observed a linear relationship (the slopes are 1.02 and 1.04 for PIDT-phanQ- and PCPDTFBT-based device, respectively) between the light intensity and short-circuit current density, suggesting that the bimolecular recombination and space charge effects can be neglected.[18,19] In addition, the light-intensity dependence PCE was also evaluated. The *J–V* characteristics of the devices were shown in Figure S2 and Figure S3 (Supporting Information). Very encouragingly, the device performance of both devices can be further increased under lower light intensity. For the PIDT-phanQ-based tandem cells, a high PCE of up to 8.5% can be reached under a light intensity of 80 mW cm^{-2} (Device G; Table 1 and Figure 2), while a PCE up to 7.9% can be reached under a light intensity of 63 mW cm^{-2} for the PCPDTFBT-based tandem cells (Device H; Table 1 and Figure 5). These results suggest that these devices can be used for indoor applications.

2.3. Semitransparent Solar Cells

The thin active layers (total thickness of 155 nm) in the tandem cell enable them to be used for making ST cell. To verify this, the device characteristics of the PIDT-phanQ-based ST cell (Device I) were evaluated. The device fabrication procedure was similar as that used for Device H, except that the thickness of the top Ag electrode was reduced to ≈10 nm. Device I exhibited a high PCE of 6.7% (light intensity = 100 mW cm^{-2}), with a J_{sc} of 5.75 mA cm^{-2}, an V_{oc} of 1.47 V, and a FF of 58.64% (Table 1 and **Figure 7**). Similar to previous tandem cells, an improved PCE (7.4%) was obtained under a low light intensity of 80 mW cm^{-2} (Device J; Table 1 and Figure 7), representing the highest value reported for a ST OPV. Moreover, Device I also possessed a high AVT (≈40%) in the range between 380 and 700 nm (**Figure 8**). The photographic image of Device I is shown in the inset of Figure 8; a University of Washington campus building can be clearly visualized through the device.

In addition to optical transmittance, suitable solar cells for window application also require good color rendering properties and transparency perception by the human eye for realistic scene illumination.[4,5] Therefore, the Commission Internationale de l'Eclairage (CIE) 1931 color coordinates, correlative color temperature (CCT), and general CRI of Device I were evaluated. Device I had a CCT of 5622 K and CIE color coordinates of (0.3297, 0.3387), which is close to AM1.5G light illumination (**Figure 9**), indicating good achromatic when looking through the device under AM1.5G illumination. In addition, Device I possessed an excellent CRI of 97.2, clearly demonstrating the exceptional color rendering properties of the device. The combined high PCE, good AVT, excellent color perception, and rendering properties of the devices enable them to be used in power-generating window applications.

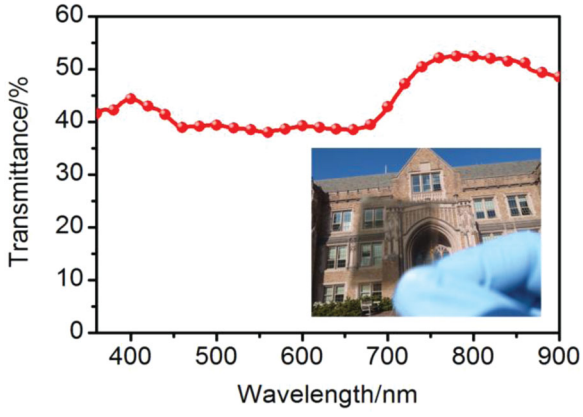

Figure 8. Optical transmittance of Device I (the description of the type of device is shown in Table 1). The inset shows a photograph of Device I.

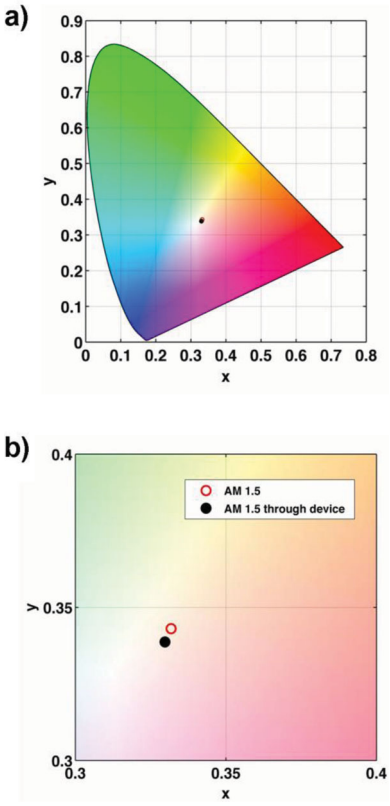

Figure 9. a) The color coordinates of Device I under AM1.5G illumination on the CIE chromaticity diagram and b) an enlarged image from (a). The color coordinate representation of AM1.5G illumination is also presented.

3. Conclusions

In summary, highly efficient tandem and ST polymer solar cells were demonstrated by utilizing the same donor polymer blended with $PC_{61}BM$ and $PC_{71}BM$ as the active layers in two sub-cells. A high PCE of 8.5% and a record high V_{oc} of 1.71 V were achieved for a tandem cell using the same medium bandgap polymer PIDT-phanQ. Similarly, a high PCE (7.9%) was obtained in a tandem cell using an LBG polymer PCPDTFBT. Due to its very thin total active layer thickness, a highly efficient ST tandem cell could also be fabricated using PIDT-phanQ as a donor; it exhibited a high PCE of 7.4%, which is the highest value reported to date for a ST OPV. This ST device also possessed a high AVT (≈40%) and an excellent CRI (97.2), which enables its use for power-generating window applications.

4. Experimental Section

Materials: PIDT-phanQ and PCPDTFBT were synthesized in-house, and the detailed synthesis was reported previously.[17,20] The number average molecular weights of PIDT-phanQ and PCPDTFBT were ≈82.4 kDa (polydispersity index = 2.42) and ≈25.3 kDa (polydispersity index = 1.5), respectively, as determined by gel permeation chromatography. $PC_{61}BM$ and $PC_{71}BM$ were purchased from American Dye Source. Unless otherwise stated, all chemicals were purchased from Aldrich and used as received.

Single-Junction Cell Fabrication: A ZnO precursor solution consisting of 20 mg mL^{-1} zinc acetylacetonate hydrate in anhydrous ethanol was spin-coated onto pre-cleaned ITO-coated glass, followed by thermal annealing in air at 130 °C for 5 min (≈20 nm). Subsequently, a C_{60}-SAM layer was deposited on ZnO using a spin-coating process as previously reported.[12] The substrates were washed with tetrahydrofuran (THF) twice to remove unbound C_{60}-SAM molecules. The active layer was then spin-cast from a solution containing a mixture of either PIDT-phanQ:acceptor (1:3 w/w) or PCPDTFBT:acceptor (1:2.5 w/w), followed by annealing at 110 °C for 5 min. The modified PEDOT:PSS layer (≈70 nm) was then spin-coated from PEDOT:PSS solution (Clevious P VP AI 4083) diluted with equal volume of isopropyl alcohol and 0.2 wt% of Zonyl FSO fluorosurfactant. Finally, an Ag layer (150 nm) was then deposited under high vacuum (<10^{-6} torr) through a shadow mask, which defined an active area of 0.036 cm^2.

Tandem Cell Fabrication: The front cells were made according to the procedure for the single-junction cell fabrication. A PH1000 layer (≈40 nm) was spin-coated onto the m-PEDOT:PSS layer from its solution (Clevious PH1000) and annealed at 120 °C for 5 min. The surface of the PH1000 layer was then washed with methanol to increase the conductivity and reduce the surface roughness as reported elsewhere.[21] Next, the rear cells were made according to the procedure for the single-junction cell fabrication. Finally, MoO_3 (7 nm)/Ag (150 nm) layers were deposited under high vacuum (<10^{-6} torr) through a shadow mask, which defined an active area of 0.036 cm^2.

Characterization: The current–voltage characteristics of un-encapsulated solar cell devices were measured under ambient conditions using a Keithley 2400 source-measurement unit. An Oriel xenon lamp (450 W) with an AM1.5 G filter was used as the solar simulator. Contributions to the J_{sc} from regions outside the active area were eliminated using illumination masks with an aperture size of 0.0314 cm^2. A Hamamatsu silicon solar cell with a KG5 color filter, which is traced to the National Renewable Energy Laboratory (NREL), was used as the reference cell. To calibrate the light intensity of the solar simulator, the power of the xenon lamp was adjusted to make the J_{SC} of the reference cell under simulated sun light as high as it was under the calibration condition. The spectral mismatches resulting from the test cells, the reference cell, the solar simulator, and the AM1.5 were calibrated with mismatch factors (M). The mismatch factor is defined as according to Shrotriya et al.[22]

$$M = \frac{\int_{\lambda 1}^{\lambda 2} E_{\mathrm{Ref}}(\lambda) S_{\mathrm{R}}(\lambda)\mathrm{d}\lambda \int_{\lambda 1}^{\lambda 2} E_{\mathrm{S}}(\lambda) S_{\mathrm{T}}(\lambda)\mathrm{d}\lambda}{\int_{\lambda 1}^{\lambda 2} E_{\mathrm{Ref}}(\lambda) S_{\mathrm{T}}(\lambda)\mathrm{d}\lambda \int_{\lambda 1}^{\lambda 2} E_{\mathrm{S}}(\lambda) S_{\mathrm{R}}(\lambda)\mathrm{d}\lambda}$$

where $E_{\mathrm{Ref}}(\lambda)$ *is* the reference spectral irradiance (AM1.5), $E_{\mathrm{S}}(\lambda)$ is the source spectral irradiance, $S_{\mathrm{R}}(\lambda)$ is the spectral responsivity of the reference cell, and $S_{\mathrm{T}}(\lambda)$ is the spectral responsivity of the test cell, each as a function of wavelength (λ). The spectral responsivities of the test cells and the reference cell were calculated from the corresponding external quantum efficiencies (EQE) by the relationship

$$S(\lambda) = \frac{q\lambda}{hc} EQE(\lambda)$$

where the constant term q/hc equals 8.0655×10^5 for wavelengths in units of meters and $S(\lambda)$ in units of A W^{-1}. The Hamamatsu solar cell was also used as the detector for determining the spectral irradiance of the solar simulator. To minimize the spectral transformation, the irradiance spectrum was calibrated with the spectral responsively of the Hamamatsu cell and the grating efficiency curve of the monochromator (Oriel Cornerstone 130). UV-Vis absorption spectra were recorded with Perkin-Elmer Lambda-9 spectrophotometer at room temperature. The optical simulations were performed based on the transfer matrix formalism.[4,23]

Supporting Information

Supporting Information is available from the Wiley Online Library or from the author.

Acknowledgements

C.-Y.C. and L.Z. contributed equally to this work. This work was supported by the AFOSR (FA9550–09–1–0426), the Office of Naval Research (N00014–11–1–0300), and the Asian Office of Aerospace Research and Development (FA2386–11–1–4072). A. K.-Y.J. thanks the Boeing-Johnson Foundation for financial support.

Received: October 29, 2013
Revised: November 7, 2013
Published online: December 12, 2013

[1] K. M. Coakley, M. D. McGehee, *Chem. Mater.* **2004**, *16*, 4533.
[2] B. C. Thompson, J. M. J. Fréchet, *Angew. Chem. Int. Ed.* **2008**, *47*, 58.
[3] S. K. Hau, H.-L. Yip, J. Zou, A. K. Y. Jen, *Org. Electron.* **2009**, *10*, 1401.
[4] K.-S. Chen, J.-F. Salinas, H.-L. Yip, L. Huo, J. Hou, A. K. Y. Jen, *Energy Environ. Sci.* **2012**, *5*, 9551.
[5] C.-C. Chueh, S.-C. Chien, H.-L. Yip, J. F. Salinas, C.-Z. Li, K.-S. Chen, F.-C. Chen, W.-C. Chen, A. K. Y. Jen, *Adv. Energy Mater.* **2013**, *3*, 417.
[6] Z. Tang, Z. George, Z. Ma, J. Bergqvist, K. Tvingstedt, K. Vandewal, E. Wang, L. M. Andersson, M. R. Andersson, F. Zhang, O. Inganäs, *Adv. Energy Mater.* **2012**, *2*, 1467.
[7] J. Y. Kim, K. Lee, N. E. Coates, D. Moses, T.-Q. Nguyen, M. Dante, A. J. Heeger, *Science* **2007**, *317*, 222.
[8] T. Ameri, G. Dennler, C. Lungenschmied, C. J. Brabec, *Energy Environ. Sci.* **2009**, *2*, 347.
[9] J. You, L. Dou, K. Yoshimura, T. Kato, K. Ohya, T. Moriarty, K. Emery, C.-C. Chen, J. Gao, G. Li, Y. Yang, *Nat. Commun.* **2013**, *4*, 1446.
[10] J. You, L. Dou, Z. Hong, G. Li, Y. Yang, *Prog. Polym. Sci.* **2013**, *38*, 1909.
[11] Y. Yao, C. Shi, G. Li, V. Shrotriya, Q. Pei, Y. Yang, *Appl. Phys. Lett.* **2006**, *89*, 153507.
[12] S. K. Hau, H.-L. Yip, O. Acton, N. S. Baek, H. Ma, A. K. Y. Jen, *J. Mater. Chem.* **2008**, *18*, 5113.
[13] S. K. Hau, H.-L. Yip, H. Ma, A. K. Y. Jen, *Appl. Phys. Lett.* **2008**, *93*, 233304.
[14] M. Lenes, L. J. A. Koster, V. D. Mihailetchi, P. W. M. Blom, *Appl. Phys. Lett.* **2006**, *88*, 243502.
[15] C. G. Shuttle, B. O'Regan, A. M. Ballantyne, J. Nelson, D. D. C. Bradley, J. R. Durrant, *Phy. Rev. B* **2008**, *78*, 113201.
[16] C.-Y. Chang, L. Zuo, H.-L. Yip, Y. Li, C.-Z. Li, C.-S. Hsu, Y.-J. Cheng, H. Chen, A. K. Y. Jen, *Adv. Funct. Mater. 23*, 5084.
[17] Y. Zhang, J. Zou, C.-C. Cheuh, H.-L. Yip, A. K. Y. Jen, *Macromolecules* **2012**, *45*, 5427.
[18] L. J. A. Koster, V. D. Mihailetchi, H. Xie, P. W. M. Blom, *Appl. Phys. Lett.* **2005**, *87*, 203502.
[19] S. R. Cowan, J. Wang, J. Yi, Y.-J. Lee, D. C. Olson, J. W. P. Hsu, *J. Appl. Phys.* **2013**, *113*, 154504.
[20] Y. Zhang, J. Zou, H.-L. Yip, K.-S. Chen, D. F. Zeigler, Y. Sun, A. K. Y. Jen, *Chem. Mater.* **2011**, *23*, 2289.
[21] D. Alemu, H.-Y. Wei, K.-C. Ho, C.-W. Chu, *Energy Environ. Sci.* **2012**, *5*, 9662.
[22] V. Shrotriya, G. Li, Y. Yao, T. Moriarty, K. Emery, Y. Yang, *Adv. Funct. Mater.* **2006**, *16*, 2016.
[23] L. A. A. Pettersson, L. S. Roman, O. Inganas, *J. Appl. Phys.* **1999**, *86*, 487.